

## Haptic forces and gamification on epidural anesthesia skill gain

André Luiz Brazil<sup>a</sup>, Aura Conci<sup>b,\*</sup>, Esteban Clua<sup>b</sup>, Leonardo Kayat Bittencourt<sup>c</sup>,  
Lúcia Blondet Baruque<sup>d</sup>, Nathalia da Silva Conci<sup>e</sup>

<sup>a</sup> Digital Games Dep., Instituto Federal de Educação, Ciência e Tecnologia, Eng. Paulo de Frontin, RJ, Brazil

<sup>b</sup> Computer Science Dep., Computer Institute, Universidade Federal Fluminense, Niterói, RJ, Brazil

<sup>c</sup> Department of Radiology, Universidade Federal do Rio de Janeiro, Rio de Janeiro, RJ, Brazil

<sup>d</sup> Digital Media Dep., Fundação CECIERJ, Rio de Janeiro, RJ, Brazil

<sup>e</sup> Health Sciences Center, Universidade Federal do Espírito Santo (UFES), Maruípe, Vitória, ES, Brazil

### ARTICLE INFO

#### Keywords:

Medical procedure  
Serious games  
Learning  
Capacity building  
Force model

### ABSTRACT

Epidural anesthesia is a blind medical procedure, where the needle insertion is a critical step. Its correct placement and location is related to the tactile perception and the loss of resistance (LOR) of tissues inside the epidural lumbar region, in order to avoid the puncture of the dura-mater membrane. Skill development and maintenance occurs through continuous practice. The main objective of this work is the development of a virtual simulator to enhance the training on the epidural anesthesia, in order to reduce the high failure rate currently reported on these medical procedures. This simulator integrates the development of the following 3 new models: (1) a force-displacement model to cover the progression of resistance forces generated by tissues along the needle insertion, based on real experiment data; (2) a force-needle model, to calculate the axial forces produced by needle deflection upon insertion, based on experiment data; and (3) a tissue model to design the thickness for each tissue on the simulator, from patient height, weight and age, based on average body measurements. The developed models added more realism when compared to previous works. The force-displacement model considers stiffness, friction and cutting forces for each tissue on epidural region, and includes a representation of needle insertion stages before and after the puncture in the behavior of each tissue. Other force models did not consider force modifiers for needle deflection before. The simulator environment implements the integration of a haptic device to control the needle movement, manipulated by the user. These devices enable to reproduce the resistance generated by the developed models providing physical feedback to user movements, to emulate sensations and reactions from the bypassed tissues (skin, fat, spinal ligaments, epidural space and dura-mater), as if those actions were executed in a real patient. The haptic device used presents six degrees of freedom (DOF), allowing translations and rotations on three axes (x, y, and z). The simulator interface was improved by incorporation of points and achievements as gamification elements to enhance the user interaction. These elements may contribute for maintenance of the trainee activity along the procedure practices, and to motivate and stimulate the student learning and skill improvement. No work have employed gamification elements on the interface of epidural simulators before.

### 1. Introduction

Several procedures in contemporaneous medicine involve the application of anesthesia, including surgery, odontology and trauma crisis, among others. In order to relief or eliminate the pain sensation, the anesthetic fluid must be administered to the patient. The location of the appliance and the appropriate use of the medical instrument are very important factors for the success of the anesthesia. Among many anesthesia forms, the epidural is the most common in obstetrics

procedures, in labor or cesarean section. Although this kind of anesthesia has been practiced for decades, the failure rates remain high (25%) [1]. Possible consequences of this failure to the patient can include from headaches to paralysis, or even death. The failure rate of these procedures can be reduced through medical training. Approaches to improve the expertise in medical procedures include watching 2D drawings and specialized videos, practice with phantoms, cadaver models, or 3D animation in virtual environment [2].

Usually, anesthesia application includes a needle insertion: a less

\* Corresponding author.

E-mail addresses: [andre.brazil@ifrrj.edu.br](mailto:andre.brazil@ifrrj.edu.br) (A.L. Brazil), [aconci@ic.uff.br](mailto:aconci@ic.uff.br) (A. Conci), [esteban@ic.uff.br](mailto:esteban@ic.uff.br) (E. Clua), [lkayat@gmail.com](mailto:lkayat@gmail.com) (L.K. Bittencourt), [luciabaruque@yahoo.com.br](mailto:luciabaruque@yahoo.com.br) (L.B. Baruque), [nath.conci@gmail.com](mailto:nath.conci@gmail.com) (N.d. Silva Conci).

<https://doi.org/10.1016/j.entcom.2017.10.002>

Received 31 May 2016; Received in revised form 5 July 2017; Accepted 6 October 2017

Available online 26 October 2017

1875-9521/ © 2017 Elsevier B.V. All rights reserved.

invasive procedure, necessary for a broad range of traditional medical treatments. It consists of injections, punctures and percutaneous treatments. The effectiveness of those are strongly dependent of needle tip position, whose accuracy improves according to the professional skill and expertise [3]. Procedure training may require 75 or more trials to acquire proficiency, a challenging number to be achieved. Most currently available simulators use phantoms: human models composed by artificial tissues, with high replacement costs. They lack visual feedback or a proper force model based on human tissues properties. Virtual simulators are already used by many medical fields of expertise, as epidural and lumbar puncture [4]. They provide an environment for unlimited experimentation, with no risks or real consequences [5], important to build and retain the skills and self-confidence necessary to the medical team.

Haptic devices present feedback to help the trainee to physically experience the sensations of modeled tissue resistances when practicing the medical procedures. The use of a haptic device may also help the practitioner to identify transitions among tissue layers and organs, as well as their nature and properties. Interactions between the needle and tissues also support the understanding of stiffness, cutting and friction mechanisms involved on a needle insertion procedure. The motivation, interest and user experience can be improved in virtual simulators. The integration of game elements into the user interface may shorten the learning time and be a more joyful experience, turning it into a serious game experience. These elements may direct and guide the trainee into the correct steps required for the procedures, provide feedback and motivate them through rewards, as points and achievements. The user performance can also be tracked and compared to the medical team.

The aim of this work is to present a virtual simulator for epidural anesthesia training, where user interaction occurs through the use of a haptic device, integrated to the developed models and interface, improved by gamification resources: an environment to add realism, motivate learning and improve medical expertise on anesthesia. The gamification includes the elements of points, achievements and levels. This work presents following sections: Section 2 includes works related to the simulation of an epidural anesthesia: explains the procedure, details the use of haptic devices, and previous works associated to force models, serious games and gamification; Section 3 details the technical novelties for the epidural anesthesia: includes force models and the thickness of epidural tissues; Section 4 includes the implementation of the virtual environment, detailing the gamification strategy employed, describing the developed prototypes and showing the results achieved from the simulator use; Section 5 focuses on conclusions and future works references.

## 2. Related work

This section describes the epidural procedure, its main steps, and comments previous works related to needle insertion experiments, force models, gamification experiences and virtual simulators already in use.

### 2.1. Epidural anesthesia procedure

The epidural anesthesia is a medical procedure to administer anesthetic fluid in a very specific region of the human body, called the lumbar epidural space. This region lies inside the vertebral column, located from two to nine centimeters below the skin [6]. Fig. 1(left) shows the lumbar epidural space region (ES).

To apply the anesthesia, first a needle must be inserted into this region, usually through the patient's back, between the L3 and L5 vertebrae, where a larger inter-vertebral space exists. The needle must pass through other tissues before reaching the epidural space. Fig. 1 (right) presents these layers: skin, subcutaneous fat (SF), supraspinous ligament (SL), interspinous ligament (IL) and ligamentum flavum (LF). The vertebrae are represented by spine process region (SP). Beyond the epidural space are the dura-mater (DM) layer, cerebrum-spinal fluid

(CSF) and spinal cord (SC). Serious damage may incur to the patient if one layer beyond the epidural space become punctured by the needle. After its placement, a catheter is introduced through the needle, in order to apply the anesthesia.

The needle insertion is a blind procedure (i.e. the physician is not able to see the interior of the patient's body). A special needle is designed for this anesthesia: the Tuohy needle (Fig. 2 - left). Its metal structure contains several markings at each centimeter, to orient the physician about the needle depth on insertion. Its plastic wings give support to the physician hands for needle guidance. Its tip is curved and beveled, to avoid the perforation of dura-mater tissue. The tissue is perforated by a second needle (thinner and sharper pointed), the mandrel, inserted inside the Tuohy needle.

The loss of resistance (LOR) technique [1,7] is used for the needle placement. It senses the resistance of the tissues bypassed by the needle along its insertion, as an orientation to detect the epidural space location (Fig. 1 - right). The LOR is used after the needle reaches the IL tissue, where the physician senses an increase on the resistance forces required for insertion. This is followed by a higher resistance increase afterwards, when the needle contacts the LF tissue, the start point for the use of LOR. When the needle reaches LF, the physician must stop the insertion and connect a saline filled syringe behind the Tuohy. The syringe is important to sense the pressure from the current tissue to saline injection. This is achieved by trying to inject the saline fluid, by pressing the plunger with the thumb and feeling the pressure resistance. A high pressure resistance to saline injection indicates that the needle is located inside LF tissue. The physician must progress slowly with the insertion and repeat the check, until a sudden drop on the pressure resistance is felt, confirming the needle arrival to the ES location.

The failure of ES detection by LOR can result in the puncture of the DM layer. The least consequence is a headache (85%) but perioperative morbidity may occur, in some cases [7]. Training can reduce the failure rate. The physician skill can be improved through direct practice on patients, guided by a senior advisor [8], although there is a shift away from this method nowadays, due to a lesser tolerance rate for errors [9]. The lack of continuous practice can also result in a significant decline on skills [10], and the use of a virtual simulator facilitates skill improvement [2].

### 2.2. Haptic devices

Haptic devices are capable of producing physical forces in resistance to the hands movement of the user. Their applications cover 3D modeling and simulations, including the use on medical procedures. It enables the sensation of immediate feedback in response to user interaction through the device, improving the realism on simulators. They may simulate tissue properties (like stiffness, damping, static and dynamic friction) and the resistance to perforation, relevant for the practice of needle insertion and epidural procedures.

The most popular haptic devices are the Phantom Omni (Fig. 3 - left) and the Novint Falcon (Fig. 3 - right). They offer different possibilities of movement (degrees of freedom - DOF). The Phantom Omni device (Fig. 3 - left) offers 6 DOF: three for axial displacements of its arm, on x, y and z axis, plus additional three, for rotations around these axis. The Novint Falcon (Fig. 3 - right) is a simplified haptic device, with 3 DOF for axial displacement, with no rotation capabilities. The use of haptic devices in a virtual simulator environment help to bridge the gap between the real world situations and the practices executed inside the virtual environment. This may result in a better user experience and increase the confidence on his skills. A Phantom Omni haptic device was integrated to the developed simulator.

The use of haptic feedback and a visual interface contribute to the needle insertion training. A study about the failure rate on needle insertions using a 2D simulator integrated to a 1 DOF haptic device has shown an improvement rate of 87% on accuracy (ex. fewer errors) on tests with a visual interface and real-time feedback, and a 52%

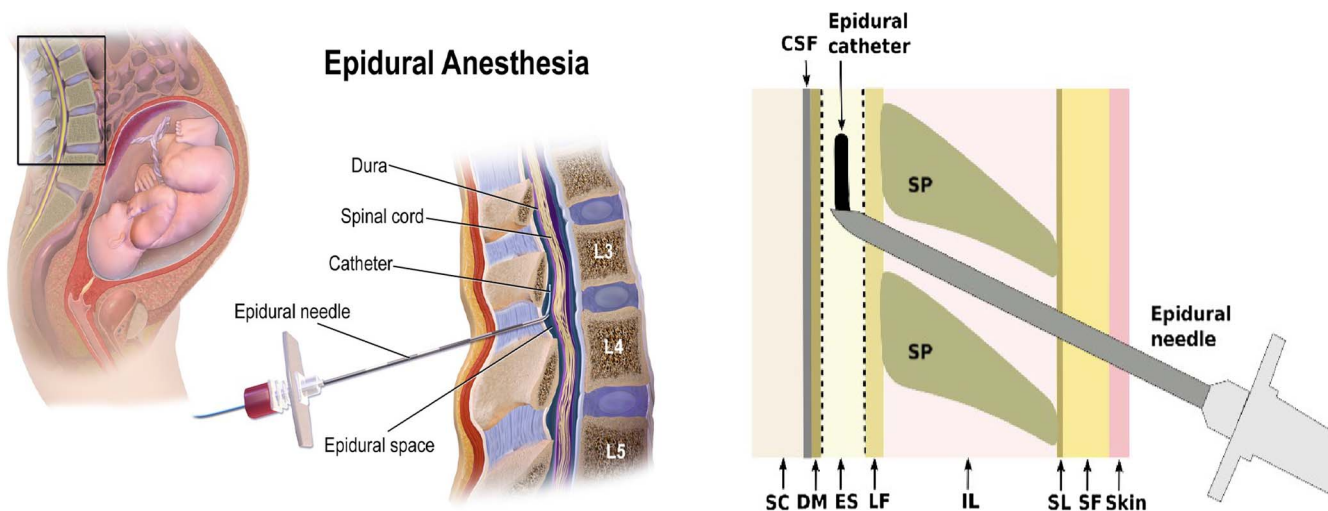


Fig. 1. Lumbar epidural space location (left) and tissues from epidural region (right).

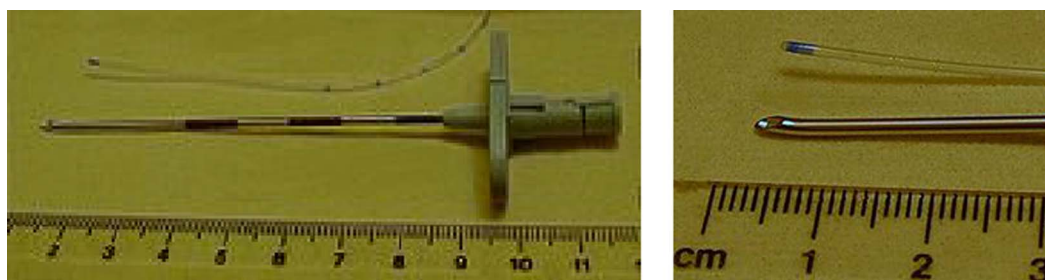


Fig. 2. A 16 gauge Tuohy needle (left) and its curved tip (right).

improvement rate when a haptic device was used for force feedback [16]. Needle insertion tasks were executed by medical trainees and also experts. Four tissues (skin, fat and muscle) and simple force calculations, combined with a dynamic and bi-dimensional interface for visual feedback were considered. These results confirm the relevance of an interface, to provide visual feedback on needle insertion simulators, and the need for haptic device feedback [16].

2.3. Needle insertion experiments and force modeling

Needle insertions on epidural anesthesia procedures are affected by biomechanical properties of the tissues [11]. The influence of stiffness, static and dynamic friction, resistance to perforation and thickness can be incorporated and used to calibrate the resistance in a virtual simulation environment.

Average force values required for human tissue perforation are  $6.0 \pm 0.7$  N (Newtons) for skin and 1.974 N for fat tissue [12]. The use of swine for biomaterials research is a common practice. Swine skin is tougher than human: experiments show an average puncture force of

$12.9 \pm 2.6$  N. Table 1 lists the epidural tissues and the average force required for their puncture based on needle insertion experiments in human and porcine [12].

Force models can be used to improve the responses in terms of haptic sensations, and better simulate the resistance on needle insertion and its movement through the tissues. The current tissue being penetrated and the needle depth are commonly used in the force model. The progression of resistance on needle insertion is associated to the needle depth on Fig. 4, where force x needle displacement curves show the tissues involved and a force drop, when the epidural space is reached [12]. The forces are higher and the muscle tissue is absent on [14] (Fig. 4 - right).

The use of curves has been associated to simulators of insertions [17–19], but these works have not designed a force model for them. A force x displacement curve from Delft University of Technology [18] is shown on Fig. 5, where the bold line shows the simulated forces, which are constant (5 Newton) until the reach of LF tissue, when it linearly rises to 16 Newton, with a sudden drop to 9 Newton on ES.

A review of epidural simulators [4] discussed a force model for



Fig. 3. Phantom Omni (left) and Novint Falcon (right) haptic devices.

**Table 1**  
Human and porcine puncture forces, steady-state forces and thickness for tissues of epidural lumbar region [12].

| Tissue                                    | Human puncture force (N) | Thickness (mm)   | Swine puncture force (N) | Swine steady-state force (N) |
|---|--------------------------|------------------|--------------------------|------------------------------|
| Skin                                      | 6.0372 <sup>b</sup>      | 10.8             | 12.9 <sup>c</sup>        | –                            |
| Fat                                       | 1.974                    | 2.8              | 6.027                    | –                            |
| Muscle                                    | 4.354 <sup>a</sup>       | 1.9              | 8.407                    | 3.675                        |
| Interspinous Ligament                     | 7.467                    | 18               | –                        | 4.053                        |
| Ligamentum Flavum                         | 12.1330 <sup>a</sup>     | 7.4 <sup>d</sup> | 6.1330                   | –                            |
| Epidural Space/Subdural Tissue/Dura-mater | 2.437                    | 8.6 <sup>e</sup> | –                        | –                            |
| Bone                                      | 8.0265 <sup>f</sup>      | –                | –                        | –                            |

<sup>a</sup> Estimated values based on swine measurements, with a correction factor calculated from swine/human tissues puncture forces.

<sup>b</sup> 6.0 ± 0.7.

<sup>c</sup> With a standard deviation of 2.6.

<sup>d</sup> 5.4 after puncture.

<sup>e</sup> 10.6 after puncture.

<sup>f</sup> The bone is impassable in this case, this is the starting force, that keeps increasing after contact.

needle insertion, and commented examples of phantom and virtual simulators. It compiled a list of desirable functionalities for an epidural simulator, considering influence factors relevant for the needle insertion.

The force model for needle insertion on soft tissues on Fig. 6 considers that an applied force ( $A_f$ ) must be superior to the resulting force ( $R_f$ ) in order to move the needle on a insertion [4,13,15]. The resulting force could be decomposed and modeled as a sum of three main forces: The stiffness force ( $S_f$ ), a resistance force derived from tissue elasticity before its perforation; the cutting force ( $C_f$ ), required force for the tip of the needle to pierce through the tissue, and the frictional force ( $F_f$ ), caused by the needle shaft rubbing on the already trespassed tissue [4,13,15]. The combination of these three main forces is the following equation:  $R_f = S_f + C_f + F_f$ . This model was based on needle insertions in bovine livers [13].

The  $S_f$  occurs when the applied force is greater than zero but the needle has not pierced through the tissue yet [4,13,15]. It increases with the applied force, forcing the needle backwards, until the force reaches a maximum stiffness value for the tissue. The tissue becomes stressed by the needle movement until the maximum elasticity is surpassed, and the tissue becomes pierced, reducing  $S_f$  to zero. Further needle movements after the tissue perforation result in frictional and cutting forces ( $F_f$  and  $C_f$ ) [4,13,15]. The  $F_f$  and  $C_f$  are only considered after the tissue puncture. The  $F_f$  uses static friction, dynamic friction and the tissue damping as calculation factors [13]. The  $C_f$  is the resistance against ripping of the tissue. It occurs only when the needle is moving inside the tissue. Needle insertions in bovine livers [13] presented an average value of 0.94 N (Newtons) with a standard deviation of 0.36 N for  $C_f$ .

The needle deflection forces are significant on needle insertions. They are influenced by both the tip type and the needle diameter [13],

where triangular (1), coned (2) and beveled (3) tips are shown on Fig. 7 (left) [15]. The needle deflection forces upon the tissues can be seen on Fig. 7 (a and b), where the forces are balanced when a symmetric tip (a) is used, while unbalanced forces are produced by a beveled-tip (b), resulting in greater needle deflection [15]. Evidence results show that needles with smaller diameters and beveled tips bend more than conical and triangular tipped ones [13].

#### 2.4. Tissue design

The thickness of tissues is another relevant aspect for modeling needle insertions. Table 2 lists the average thickness of epidural tissues and the needle depth required to reach them, based on needle insertion experiments in human and porcine [19].

The skin tissue thickness is also related to the subscapular skinfold (SS) thickness, another common measurement usually applied to estimate patients' body fat percentage. Fig. 8 shows the SS region and its measuring procedure. The SS thickness could be estimated, based on average values for waist dimensions and the body mass [18]. Tables 3 and 4 lists some average values for these parameters obtained from American women versus age range [19]. A correlation between the waist circumference size and muscle tissue thickness was also perceived on experiments [20].

#### 2.5. Serious games and gamification

Standard simulators can take advantage of gamification strategies to engage the users by transformation of the virtual environment to improve the motivation and frequency of their use. The games are “teaching players to deal with several situations and problems in an efficient way, helping them into finding good solutions, developing

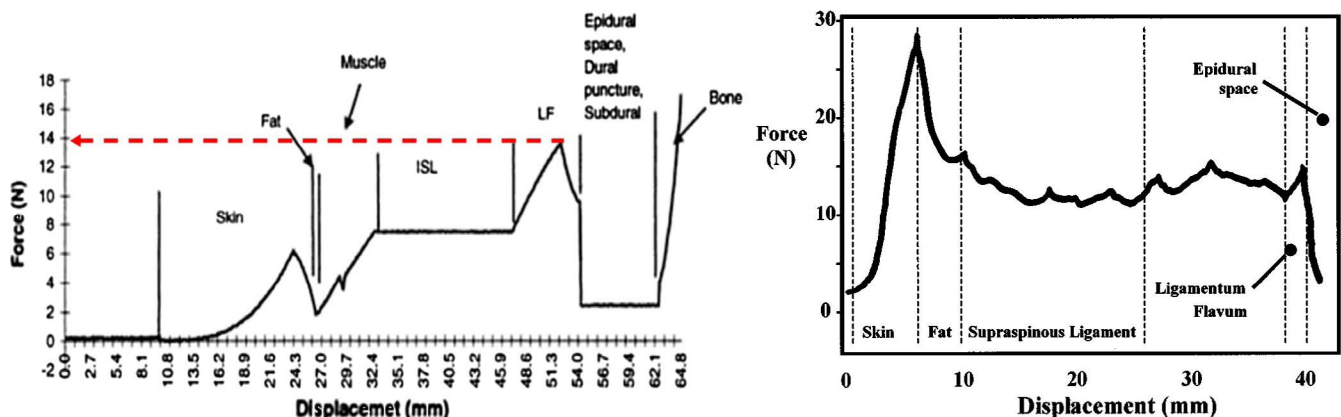


Fig. 4. Force x needle displacement curves in epidural region: [12] (Left) and [14] (Right).

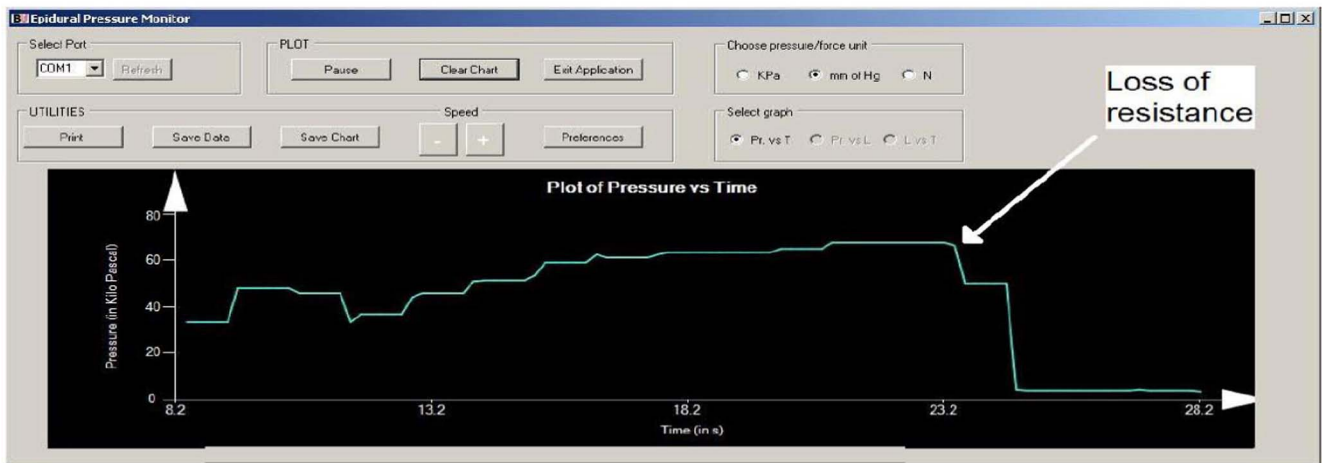
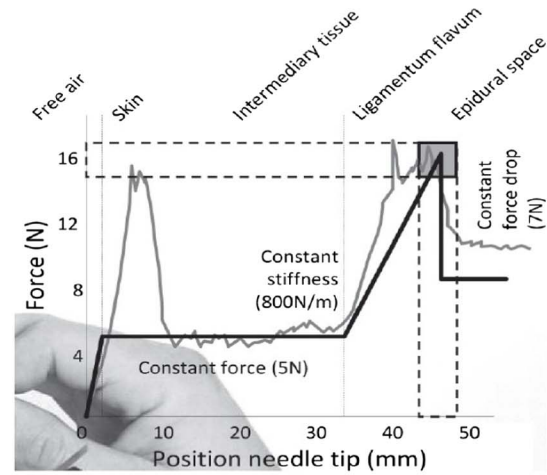
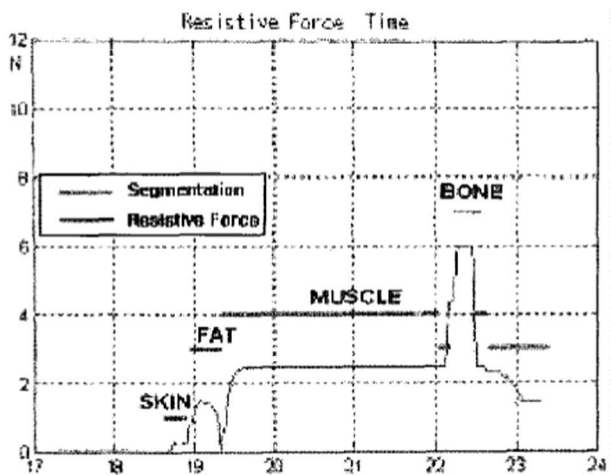


Fig. 5. Force x displacement curves, from Delft University of Technology epidural simulator [18]

Fig. 6. Main elements and forces involved in needle insertion procedure [4,13,15].

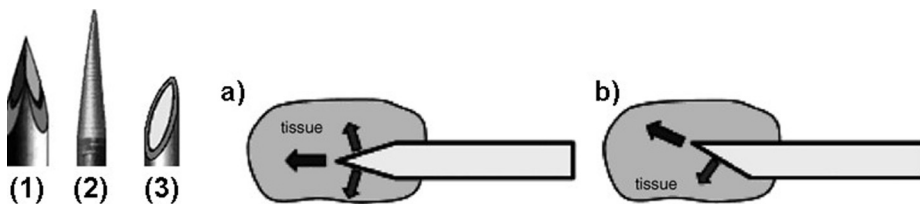
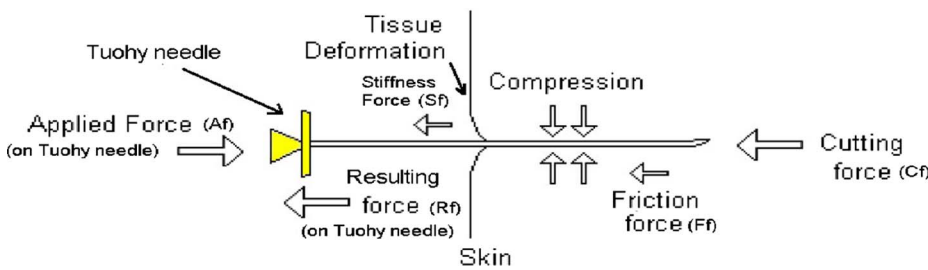


Fig. 7. Needle tip types (left): triangular (1), Coned (2) and beveled (3), and the needle deflection forces produced by a symmetric tip (a) and beveled tip (b).

quick reflexes and organize, collaborate and act more effectively in a team” [21]. Millions of youngsters, teenagers and adults confirm the power and influence exerted by the games among their quotidian life. Computer games are able to put the individual in the center of the activity, and a motivation to play comes from the possibility to change the game outcome and its results through the player’s actions [22]. The gamification seeks to take advantage of this game scenery. It comes as a “translation” or adaptation of game elements, so these resources could

be applied in other processes and contexts, beyond the game environment [24], including improved services that incorporate *gameful* (ludic and meaningful) features [23]. The gamified environment is usually less immersive than a game, but coexists with everyday life. The objectives inside the first are usually associated or affect to the execution of tasks in the second.

The most common elements present in games and gamification processes are the points, badges and leaderboards (Fig. 9). They

**Table 2**  
Average thickness, depth and needle insertion forces, based on porcine and human measurements [19].

| Porcine Tissue Layer | Tissue Thickness (mm) | Needle Depth (mm) | Insertion Force (N) |
|----------------------|-----------------------|-------------------|---------------------|
| Skin                 | 3                     | 0                 | 12.9                |
| SF                   | 6                     | 3                 | 6                   |
| SL                   | 4                     | 9                 | 9                   |
| IL                   | 26                    | 13                | 8                   |
| LF                   | 3                     | 39                | 11.1                |
| ES                   | 6                     | 42                | 0                   |
| DM                   | 15                    | 48                | 2.0                 |

compose a popular gamification strategy (PBL) [25], where the points may be used to indicate the user experience, the badges are usually associated to achievements and reputation, and the leader board promotes action by competition. Additional elements include levels and progress bars.

The “achievements” is another gamification resource to engage the user. They integrate objectives and instructions usually associated to reputation and status gains. An example of its use is a mobile application directed to encourage the exploration and recognition of a university campus by newcomers [26].

Practice guidelines for gamification implementations [23] include the use of significant elements, its proper orientation towards inspiring actions and the preservation of user autonomy on decision taking, where the outputs of a gamified environment itself could be an indicator of the users preferences [24].

Serious games, on the other hand, can be defined as games with a specific purpose, mainly targeted for learning and training. Fig. 10 shows examples of medical games associated to the use of X-ray and magnetic resonance imaging (MRI) medical fields for learning. Other knowledge topics, as ultrasound, computer tomography (CT), pathology, and cardiology are also being adopted.

Corporative, academic and scientific society fields are incorporating serious games and gamification practices in their environments, where studies show the gamification is capable to encourage and engage individuals toward objectives and ideals [26,28].

Investigated gamification experiences on the medical field included the practice of minimally invasive surgeries in a simulator by urology residents in USA [10], where the use of points, a leader board and financial rewards boosted the average amount of time spent by each user on simulator training from 2.7 to 83.9 hours per month, with the gamification. The importance of regular procedure training to improve and maintain the skill level of the residents is described as well [10].

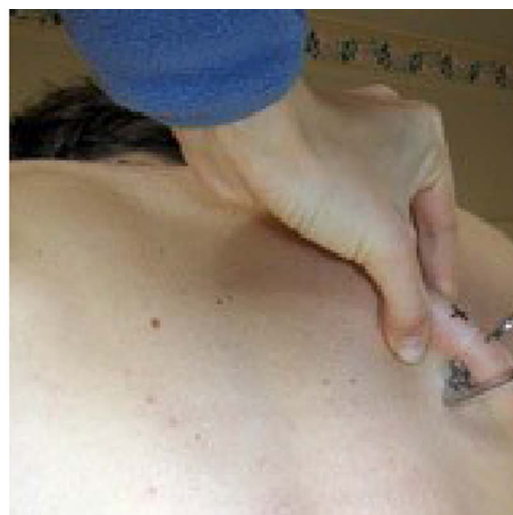
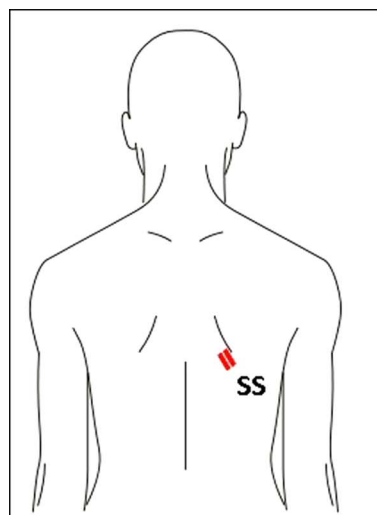


**Fig. 8.** Subscapular Skinfold (SS) Region (left) and its measurement procedure (right).

**Table 3**  
Average female body area circumferences [18].

| Body Cross-section Area | Range (cm) | Circumference (cm) | Area (cm <sup>2</sup> ) | (%) of total body area |
|-------------------------|------------|--------------------|-------------------------|------------------------|
| Waist                   | 60–120     | 85                 | 574.94                  | 31.81                  |
| Hip                     | 80–130     | 100                | 795.77                  | 44.02                  |

**Table 4**  
Mean body mass, height and body-mass index from American population (1999–2002) [19].

| Age   | Body mass (kg) | Height (cm) | BMI (kg/m <sup>2</sup> ) |
|-------|----------------|-------------|--------------------------|
| 20–29 | 71.1           | 162.8       | 26.8                     |
| 30–39 | 74.1           | 163.0       | 27.9                     |
| 40–49 | 76.5           | 163.4       | 28.6                     |
| 50–59 | 76.9           | 162.2       | 29.2                     |
| 60–74 | 74.9           | 160.0       | 29.2                     |
| 75+   | 66.6           | 157.4       | 26.8                     |

Another class of gamification included the use a haptic device for stroke rehabilitation [27], where a patient must lift and maintain a metal pole in a horizontal position, with use of all members: arms, hands, shoulder and muscles structure, so a weak shoulder could be exercised with the help of a strong one. A position tracking device installed on the pole linked to a game interface with points improves the feedback and recording capabilities when compared to other training exercisers.

Corporative experiences include the gamification of the IBM's social network [28], used by more than 400 thousand employees over the world, where the use of points, titles and a leader board intensified the network activity, and resulted in a 40% increase on communication and posts, along eleven months. The reputation, the social interaction and the competition were the most important motivational factors.

These investigated experiences show that gamification is an interesting approach to maintain user practice for a longer time, once many attempts of epidural anesthesia are normally required to improve the medical skill and proficiency, necessary for the procedures, preferably before real interactions with patients.

### 3. Technical novelties

This section presents four models developed to improve the needle insertion in the simulator. The first two (Section 3.1) represent the resistance forces generated by tissues on needle insertion. The third



Fig. 9. The PBL game elements: badges (left), and a leader board (right), listing the score (points) of best players. Fonts: talentim.wordpress.com/category/innovation (left). blog.evanoxfeld.com/gamification-intro-presentation/ images/gameon\_leaderboard.png (right).

model (Section 3.2) maps the axial forces involved in the needle deflection, and the fourth model (Section 3.3) calculates the thickness for each epidural tissue on the simulator. All of them are based on experiment data.

3.1. Force models for tissue resistance

Previously presented force models employed fewer constants to represent tissue properties and forces in a needle insertion, resulting in a lesser accurate force simulation, or its application is limited to few specific tissues or situations.

The following models consider each tissue on epidural region, includes the stiffness, friction and cutting forces, and subdivide the needle insertion on each tissue in two stages: before and after the puncture. These models enable a better simulation of biomechanical forces and their application on a virtual environment, turning the needle insertion a more realistic experience. To represent tissue behavior before puncture, Eq. (1) is proposed:

$$R_f = S_f = a_0 + (a_1 * \Delta d) + (a_2 * \Delta d^2) + (a_3 * \Delta d^3) \tag{1}$$

In (1),  $a_0$ ,  $a_1$  and  $a_2$  are constants that reproduce the resistance of the tissue currently on the needle tip (i.e. before being penetrated), where values are shown on Table 5. The  $\Delta d$  represents the needle displacement, calculated as the current needle tip depth (in millimeters) minus the depth of first contact location between the outermost tissue and the needle. Ex: For the skin tissue  $\Delta d$  is the needle displacement from needle tip to the point where the skin was first contacted. Most tissue

Table 5  
Tissue force parameters before tissue puncture.

| Tissue          | $a_0$ (N) | $a_1$ (N/m) | $a_2$ (N/mm <sup>2</sup> ) | $a_3$ (N/mm <sup>3</sup> ) | Max. Stiffness Force (MSF) (N) |
|-----------------|-----------|-------------|----------------------------|----------------------------|--------------------------------|
| Skin            | 0.0235    | 0.0116      | -0.0046                    | 0.0025                     | 6.0372 N                       |
| MS              | 1.9736    | 0.8287      | 0.1078                     | 0                          | 4.354 N                        |
| IL              | 4.4062    | 0.9598      | 0                          | 0                          | 7.467 N                        |
| LF <sup>a</sup> | 4.533     | 1.5029      | -0.0583                    | 0                          | 12.1330 N                      |
| ES              | 2.437     | 0           | 0                          | 0                          | 2.436 N                        |
| Bone (Strike)   | 3.9735    | 2.210       | 1.4814                     | 0                          | 50 N                           |

<sup>a</sup> Values adjusted to represent tissue behavior reported on Fig. 4.

data provided on Table 5 were obtained from experiments [12]. The values for LF were adjusted for better simulation of this tissue behavior.

After a tissue puncture,  $R_f$  (Resulting force) =  $F_f + C_f$  (Friction force + Cutting force). The resulting force formula uses different constants. The reaction of tissues after perforation is represented by Eq. (2).

$$R_f = F_f + C_f = ap_0 + (ap_1 * \Delta dp) + (ap_2 * \Delta dp^2) \tag{2}$$

In (2),  $ap_0$ ,  $ap_1$  and  $ap_2$  are constants that reproduce current tissue behavior after puncture, according to the Table 6,  $\Delta dp$  represents the needle depth after tissue puncture, being calculated as the current needle tip depth (in millimeters) minus the needle depth of puncture location of the outermost tissue. For instance, on the skin tissue  $\Delta dp$  is the needle displacement from needle tip to the point where the skin was first punctured. Table 6 data were mostly obtained from experiments

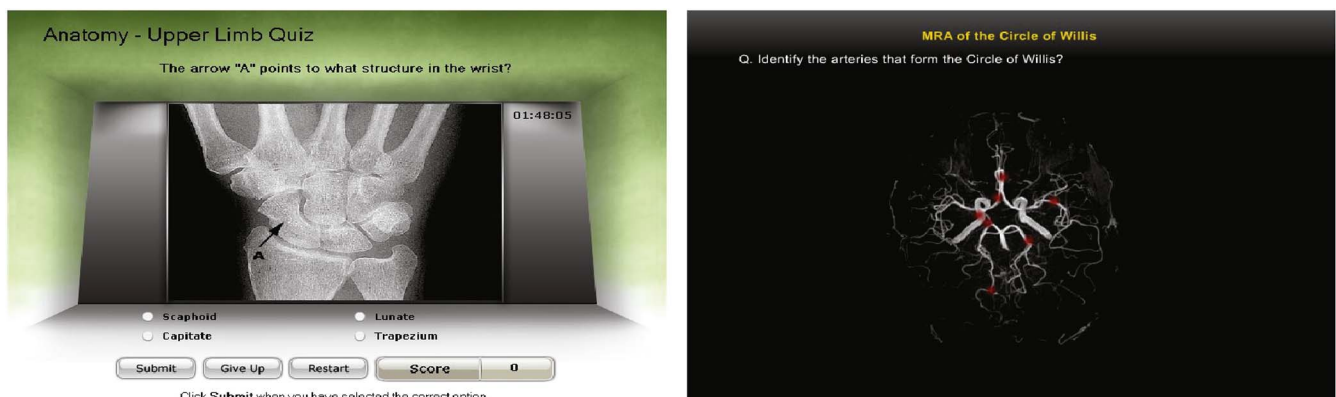


Fig. 10. Examples of medical games: X-ray (left) and MRI (right): Philips Learning Connection [26,28] Font: <http://www.theonlinelearningcenter.com/free-online-medical-games.aspx>.

**Table 6**  
Tissue force calculation parameters after tissue puncture.

| Tissue          | ap <sub>0</sub> (N) | ap <sub>1</sub> (N/mm) | ap <sub>2</sub> (N/mm <sup>2</sup> ) | Thickness (mm) | Transition Force (N) |
|-----------------|---------------------|------------------------|--------------------------------------|----------------|----------------------|
| Skin            | 6.0372              | 0.4516                 | -0.5287                              | N/A            | 1.974 N              |
| MS              | 4.354               | -2.2543                | 0.2902                               | N/A            | 3.675 N              |
| IL              | 7.467               | 0                      | 0                                    | 18 mm          | N/A                  |
| LF <sup>a</sup> | 12.1330             | -0.1693                | -0.1177                              | 7.4 mm         | N/A                  |
| ES              | 2.437               | 0                      | 0                                    | 8.6 mm         | N/A                  |
| Bone            | N/A                 | N/A                    | N/A                                  | 10 mm          | N/A                  |

<sup>a</sup> Values adjusted to represent tissue behavior on Fig. 4.

[12], with values adjusted to better represent the LF tissue behavior. The stage transition before puncture to after puncture occurs after  $R_f$  achieves the maximum stiffness force (MS<sub>f</sub>) for the tissue (Table 5). The transition between the current tissue and next tissue occurs after  $\Delta dp$  surpasses the tissue thickness (in millimeters), or the resulting force is lower than the tissue transition force (T<sub>f</sub>), whichever occurs first.

The resulting forces from the two equations were recorded and plotted together in a force x needle depth graph (Fig. 11). It shows the forces acting in skin, SF, MS, IL, LF, ES and bone. The simulation results and curve behavior are close to the data obtained for porcine and human needle insertion experiments from Fig. 4 [12], where plotted data consider that tissue contact with the needle starts at 10 mm.

Comparison tests have shown two inconsistencies on [12]. A perforation force of 12.1330 N was indicated on [12] for LF tissue, while their curves representation have shown a different perforation value (around 14 N) associated to this tissue, as indicated by the traced arrow, visible on Fig. 4. The second issue was related to a quick force decay of the post-puncture force function for LF from [12]. The use of these values do not corresponded to the descendant curve for LF as shown on Fig. 4. They needed to be adjusted, in order to better reproduce the curve displayed for LF. The updated values are listed on Tables 5 and 6, with the resulting forces being plotted on Fig. 11.

These equations were also used on a comparison with experiments plotted on Fig. 12 (Left) [13]. The original and adjusted constant values for the tissues are listed on Table 7, where adjusted values appear on the column 3. The results are plotted on a force x displacement graph (Fig. 12 - right) that includes distinct curves for the stiffness, friction, cutting and resulting forces. The resulting force follows the trajectory and values of “Model” line shown on Fig. 12 (Left).

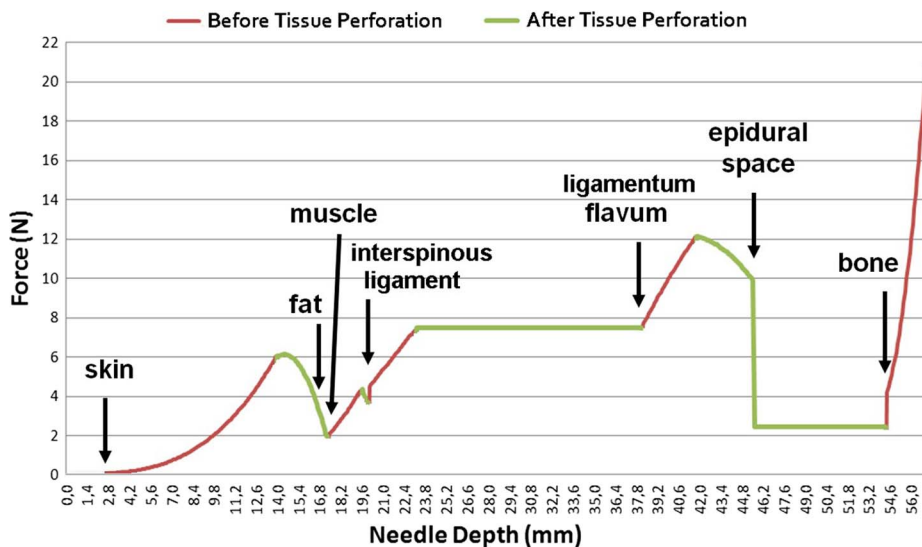


**Fig. 11.** Needle force x depth curves by simulation model (prototype 3) for all tissues in epidural anesthesia procedure.

### 3.2. A force model for needle deflection

Previous works presented needle deflection experiments and results, but do not develop an equation to calculate the deflection forces involved on a needle insertion. A needle deflection model adds realism on needle insertion simulations, once it accounts for needle-tissue forces related to the advancement of the needle do not in a straight line. This developed model considers both the tip type and the needle diameter as parameters for needle deflection. Its results can be stacked to the models developed on Section 3.1, to consider both the resistance and deflection forces on a needle insertion simulator.

Needle deflection occurs when the tissue around the needle tip is compressed and exerts an unbalanced force against this compression, depending on the tip format. The axial forces associated to the needle deflection ( $D_f$ ) are mapped by the equations:

$$\begin{aligned}
 D_f &= (-0.1953*N_d - 0.05948)*\Delta d/2.65 \text{ (for needle type 3), or} \\
 D_f &= (-0.2963*N_d - 0.08019)*\Delta d/2.65 \text{ (for needle type 4), or} \\
 D_f &= (-0.2665*N_d - 0.05539)*\Delta d/2.65 \text{ (for needle type 5)}
 \end{aligned}
 \tag{3}$$

Three factors are considered on  $D_f$  calculation:  $N_d$  is the needle diameter (the gauge, in millimeters),  $\Delta d$  is the needle depth (in millimeters), and the type of the needle tip (3, 4 or 5). For the tip type of the needle, Number 3 corresponds to a triangular tip, Number 4 represents a coned tip, and Number 5 stands for a beveled tip, the most common tip type used on epidural procedures, to avoid an accidental perforation of DM tissue.

Eq. (3) were generated from linear regressions produced by the use of MATLAB® Software, using experiment data [13]. Fig. 13 shows a linear regression graphic sample executed on the Curve Fit feature for the beveled tip type (5).

### 3.3. Dimensioning the thickness of epidural tissues

Considering average of previous mentioned data represented on Tables 2–4 [20], a model to estimate the tissues thickness as a function of the waist dimensions, age and body mass was developed. The developed model devises a strategy to estimate the thickness of all tissues in the epidural region, based on average values of female waist, tissue thickness, patient age and mass. The objective is to enable the generation of different patient models for training in the epidural simulator, based on an input data of a patient age and weight values, to improve its possibilities and the challenges for the user. The following equation can calculate the tissue thickness:

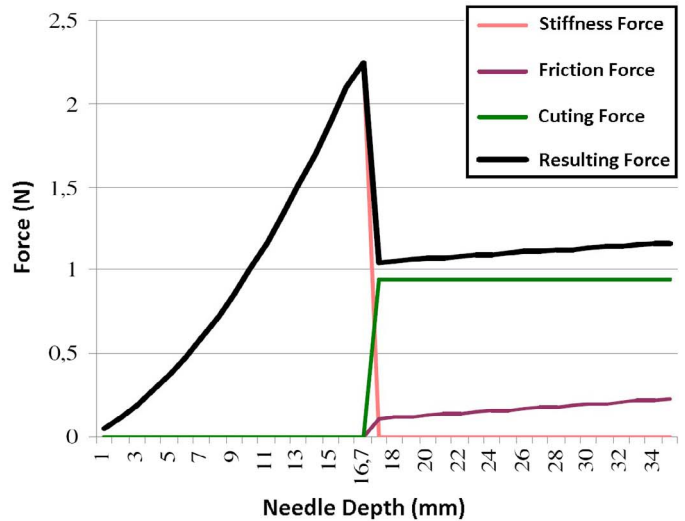
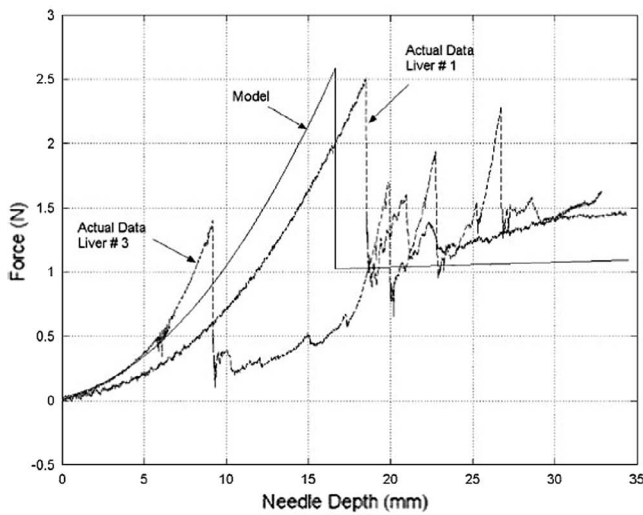


Fig. 12. Left: Force × displacement curves for needle penetration [13]. Right: Corresponding curves (Newtons) × displacement (in mm) by simulation model.

Table 7 Measures from bovine liver tissues and values used and obtained in simulation model.

| Parameter                   | Tissue 1 | Tissue 2 | Values used in implemented simulation |
|-----------------------------|----------|----------|---------------------------------------|
| $a_1$                       | 0.0480   | 0.0020   | 0.0480                                |
| $a_2$                       | 0.0052   | 0.0023   | 0.0052                                |
| MSf (N)                     | 2.3040   | 1.4000   | 2.2410                                |
| Puncture depth ( $d$ ) (mm) | 16.6514  | 15.0000  | 16.6514                               |
| $R_f$ (after puncture) (N)  | 0.6579   | 0.9000   | 1.0472                                |

$$T_t = \left( \frac{\sqrt{(A_w \times (B_m/A_m)) / \pi}}{R_w} \right)^3 \times A_t \tag{4}$$

where  $B_m$  is the body mass (in kg) for the patient to be generated.  $A_m$  is an average body mass for a patient based on a given age, where reference values can be found on Table 9.  $A_w$  is the average waist area for women, where values are shown on Table 8.  $R_w$  is the waist radius, calculated as  $\sqrt{A_w/\pi}$ .  $A_t$  is an average thickness value for a given tissue, where values are located on Table 2. These factors are combined to determine  $T_t$ , the thickness (in millimeters) of a tissue for a given patient.

For example, these reference values could be used:  $A_m$  (average mass) = 71.1 kg for a 20–29 years average female (Table 4),  $A_w$  (average waist area) = 574.94 cm<sup>2</sup> (Table 3),  $R_w$  (average waist radius) = 13.5280 cm, and  $A_t$  (average thickness) = 3 mm for skin tissue. This model uses waist data from female due to a more frequent use of

Table 8 Average female body area circumferences [18].

| Body Cross-section Area | Area (cm <sup>2</sup> ) | (%) of total body area |
|-------------------------|-------------------------|------------------------|
| Waist                   | 574.94                  | 31.81                  |
| Hip                     | 795.77                  | 44.02                  |

Table 9 Mean body mass, height and BMI from American population (1999–2002) [19].

| Age   | Body mass (kg) | Height (cm) | BMI (kg/m <sup>2</sup> ) |
|-------|----------------|-------------|--------------------------|
| 20–29 | 71.1           | 162.8       | 26.8                     |
| 30–39 | 74.1           | 163.0       | 27.9                     |
| 40–49 | 76.5           | 163.4       | 28.6                     |
| 50–59 | 76.9           | 162.2       | 29.2                     |
| 60–74 | 74.9           | 160.0       | 29.2                     |
| 75+   | 66.6           | 157.4       | 26.8                     |

epidural procedures on women, but data from males could be used as well. This example considers average skin tissue thickness ( $A_t$ ) and relates to an average waist size and mass, in order to obtain skin tissue thickness ( $T_t$ ). Subscapular skinfold (Fig. 8) measurements involve tissue thickness (doubled/folded) together with subcutaneous fat and were used as a reference. Experiment data only covers a correlation between body dimensions and skin, fat and muscle tissues. This idea was extended for other internal tissues from epidural region, using the average thickness data from Table 2, where further validation would be

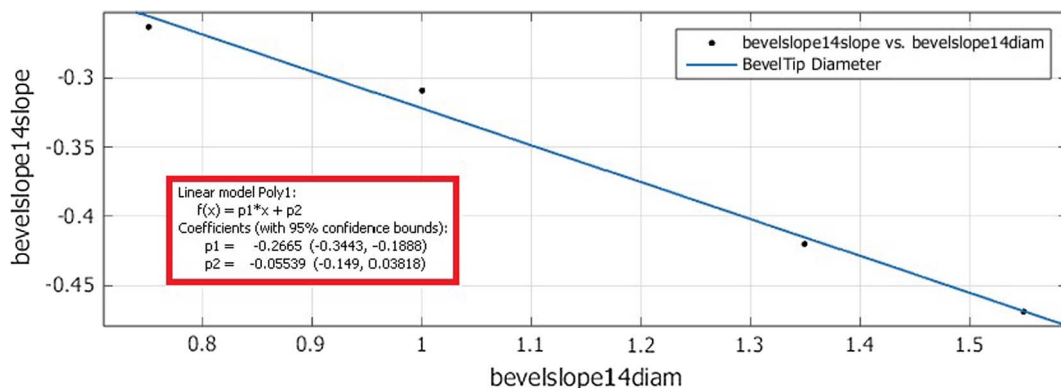


Fig. 13. A linear regression graphic, generated with the Curve Fit feature of MATLAB® Software.

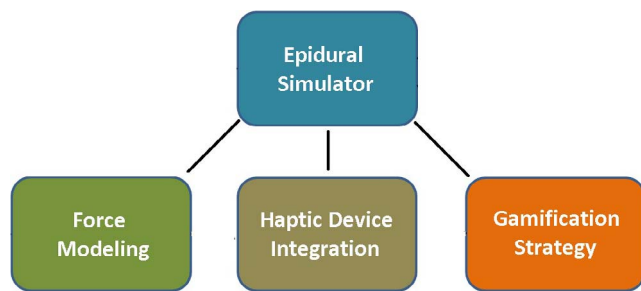


Fig. 14. The three main features on the epidural simulator.

recommended.

#### 4. Implementation novelties

This section includes developed strategies related to the virtual simulator for epidural anesthesia and the features incorporated to its interface and environment. It includes a gamification strategy to engage and motivate the users.

##### 4.1. The epidural simulator

A virtual simulator is implemented for the practice of needle insertion on epidural anesthesia procedure. It incorporates and adjusts the force models developed on Section 3. It integrates the use of a haptic device for interaction and some gamification elements, to improve the realism and provide a better motivation to the users. Fig. 14 presents the three main aspects integrated to the development of the virtual environment. A secondary objective of this implementation is to create a lower cost training solution, once the equipment for medical procedures practice is very expensive and usually involves the use of phantoms with a limited lifespan, and a permanent cost for parts replacement.

The implementation uses the Unity3D engine. It includes a facility to import and integrate 3D models, useful to speed up an initial setup for the training environment, and allows the development of programming scripts using C#, JavaScript and Python languages. C# was used to integrate the force models from Section 3 into the simulations. This engine also have a strong and active online community of developers, and offers a free cost (Personal) version, with the option of publishing the implemented solution to personal computers (PCs) and other mobile platforms, as Android and IOS.

##### 4.2. The gamification strategy

The gamification strategy for the virtual simulation environment uses points and achievements. The use of points is incorporated to the tutorial mode of the prototype (Fig. 16).

The use of achievements is relevant to motivate the users on simulator practices, providing feedback of concluded objectives and to be used as a measurement of reputation. They are useful to orient the trainees about the remaining tasks needed to complete the entire needle insertion step on the epidural procedure, and engage them to accomplish the whole practice, by conclusion of all proposed achievements.

The use of points associated to the achievements help into the evaluation of each part of the procedure. They enable a quantitative tracking of the user progress in the simulator, as well as a performance registry and a further comparison of the obtained results between the user and his colleagues. Negative points were not applied, because they would cloud the tracking mechanic for the user progression.

A list of achievements of the simulator environment is detailed in Table 10. These were subdivided two modes: a tutorial mode and the simulation mode. The tutorial mode is focused into scaffolding of the user with the simulator use, and the needle manipulation in the

Table 10  
Achievements list and its associated points.

| Mode       | Achievement   | Points Awarded |
|------------|---|----------------|
| Tutorial   | Penetrate skin tissue   | 100            |
| Tutorial   | Identify L3 vertebra  | 100            |
| Tutorial   | Identify L4 vertebra  | 100            |
| Tutorial   | Locate epidural space   | 500            |
| Tutorial   | Locate and perforate dura-mater layer   | 250            |
| Simulation | Locate skin region between L3 and L4 vertebrae                                    | 300            |
| Simulation | Penetrate skin region between L3 and L4 area                                      | 500            |
| Simulation | Penetrate muscle tissue in the right area   | 700            |
| Simulation | Achieve supraspinous ligament between L3 and L4 vertebrae                         | 1000           |
| Simulation | Insert the needle inside ligamentum flavum  | 1500           |
| Simulation | Detect and enter in the epidural space layer without perforating dura-mater layer | 3000           |

simulator by interaction with the haptic device. The simulation mode is directed to the needle insertion procedure: it includes all the epidural tissue layers to be penetrated by the needle until the arrival to the epidural space.

##### 4.3. The implementation details and results

The 3D model used for the virtual patient in the environment (Fig. 15) included a woman trunk, with a resolution of 10 k polygons, generated with help of Fuse software™. A deformation effect was added for the skin tissue upon needle contact, by the use of the interactive cloth component available in the development engine, to increase the visual realism of the simulation.

The tutorial mode (Fig. 16) was developed to improve the familiarity with the haptic device, so the user could feel and understand the resistance involved in the simulator environment. The needle movement was controlled by the user, through the handling of the haptic device. The user was challenged to interact with the tridimensional trunk: insert the needle through the skin tissue (the other tissues were not enabled in this mode) and move the needle up to the locations of L3 and L4 vertebrae inside the virtual patient body, virtually “touching” them and identifying their location. Small purple spheres were added to the 3D environment to indicate and facilitate the vertebrae location. The intention was to prepare the user for a further needle insertion into the inter-vertebral space, and the penetration in the interspinous ligament.

The gamification implemented for the tutorial mode included the elements of points and achievements. The configured achievements included a total of three tasks, including the skin penetration and both vertebrae identification, each tied to a 100 points reward upon its

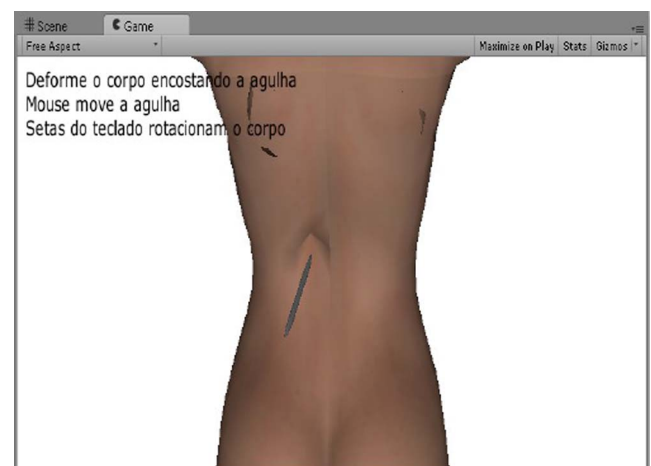


Fig. 15. The woman 3D trunk with a skin deformation.

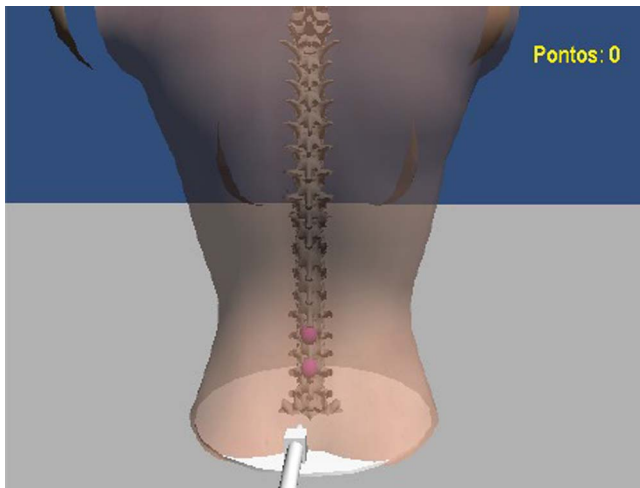


Fig. 16. The interface of tutorial mode.

conclusion. The user total score was displayed in the upper right part of screen interface. A feedback sound effect was also incorporated when the user “touched” each correct vertebra with the needle (L3 and L4). A background music with a medical ambient theme was included too.

The simulation mode included the force models from Section 3, with force components and real time force calculation capabilities. It was important to verify the possibilities of the developed equations for modeling a more realistic behavior integrated to a haptic system, capable to provide sensations in response from the user actions, and reactions from the device along the needle insertion. It considered the contact and penetration of different tissues involved into the epidural anesthesia. A left-side view of this mode in a low resolution is visible on Fig. 17 (left). A high resolution 3D view is available on Fig. 19, where is possible to visualize the current tissue (layer) being perforated as well as current needle depth. An online demonstration video for the needle insertion in the simulator is available at: <https://youtu.be/OmdwvFio8Rs>.

The implementation of the needle insertion in the simulation mode after the tissue perforation included both the movement restrictions and the corresponding haptic sensations as feedback. Each time the needle contacts the skin surface, a virtual ray is traced to the interior of patient body, to define a puncture direction. This ray is used as a resource to

trace a directional path for the needle insertion, in order to implement the movement restrictions and a maximum depth for the insertion. The start point for the ray is the contact point between the skin surface and the needle. The direction of the ray is based on the current tip orientation of the pen attached to the haptic device (the outermost part of it, on Fig. 3). Movement restriction forces are applied as the needle deviates from the direction path initially traced by the ray on its insertion. The integration with the haptic device was facilitated by a communication plugin [29], with functions for reading the updated position and orientation of its pen tip.

The visual interface of the simulator mode was implemented to take into consideration the needle penetration through the internal tissues located on the epidural region. The skin, subcutaneous fat, muscle, interspinous ligament, ligamentum flavum, epidural space and bone tissues were all visually represented by cylindrical-based shapes, generated with the engine resources. Textures obtained from real tissues samples were applied to the shapes, to increase the simulation realism. Texture samples of skin, subcutaneous fat and muscle tissues can be visualized on Fig. 19. A transparency effect was applied on each tissue after the needle contact. A text panel display is located on the top-right side of screen to show details about the needle configuration parameters, as the tip type and diameter, as well as the updated data force values for the current tissue under penetration. A 3D model for a Tuohy Needle was incorporated (Fig. 18 - right).

An interface comparison between the implemented simulation mode and the 2D needle insertion simulator from [16] can be visualized on Fig. 17. The simulator on [16] used an 1 DOF haptic for user feedback, and only displayed the skin, fat, muscle and bone tissues as simple geometric figures. Both interfaces offer detailed force data about the needle insertion. The implemented simulator displays more details about the needle use, including information about its tip type and diameter.

An editor mode was also implemented, for configuration of the biomechanical properties from the epidural tissues. The editor interface includes sliders for the adjustment of the properties values for: static friction, dynamic friction, stiffness, resistance to perforation, damping, punctured static and dynamic friction (Fig. 19). The OpenHaptics Toolkit [11] was used to implement the haptic device simulation of the tissue properties on the physical hardware.

The developed simulator was presented to a medical senior for feedback, concerning the virtual environment use for the practice of the needle insertion. He considered the implemented features as important

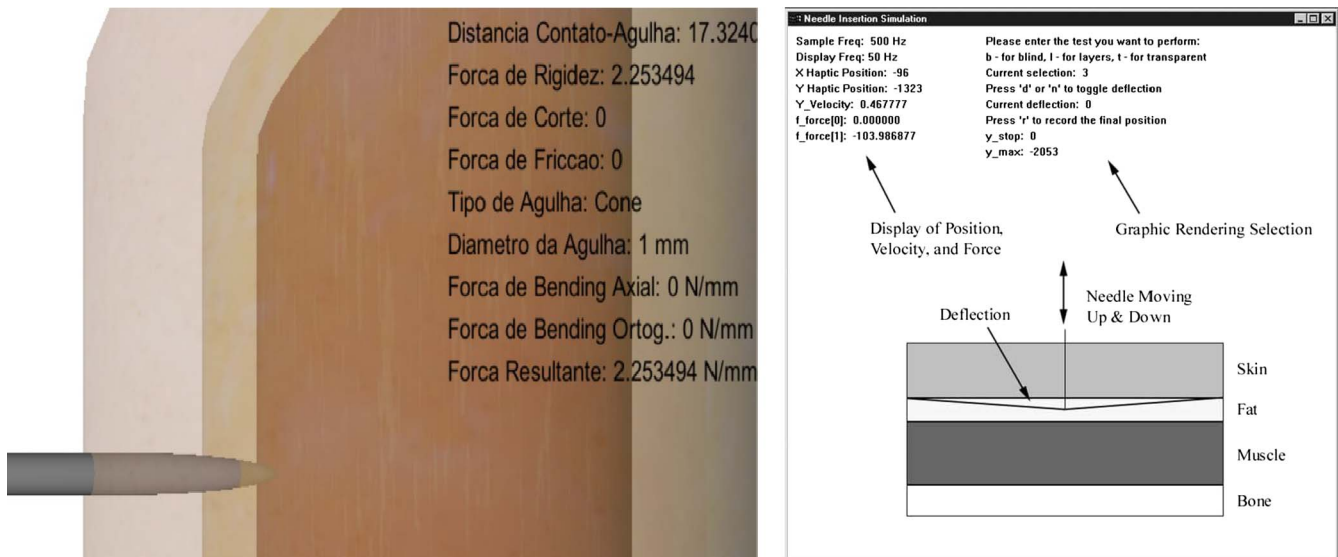


Fig. 17. A comparison of simulator interfaces: the developed implementation (left) and [16] work (right).

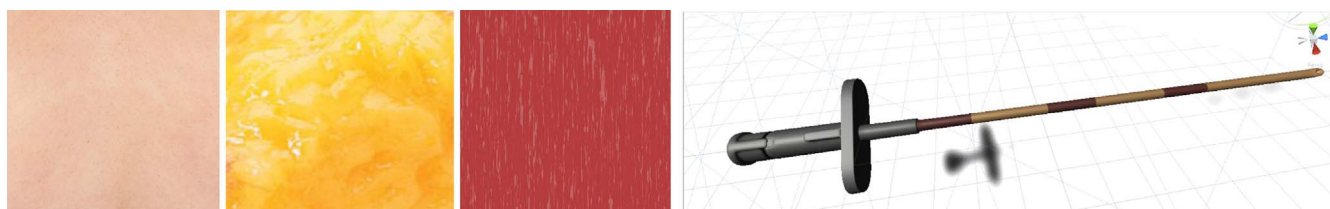


Fig. 18. Textures samples from real tissues (left) and the 3D model of a Tuohy needle (right).

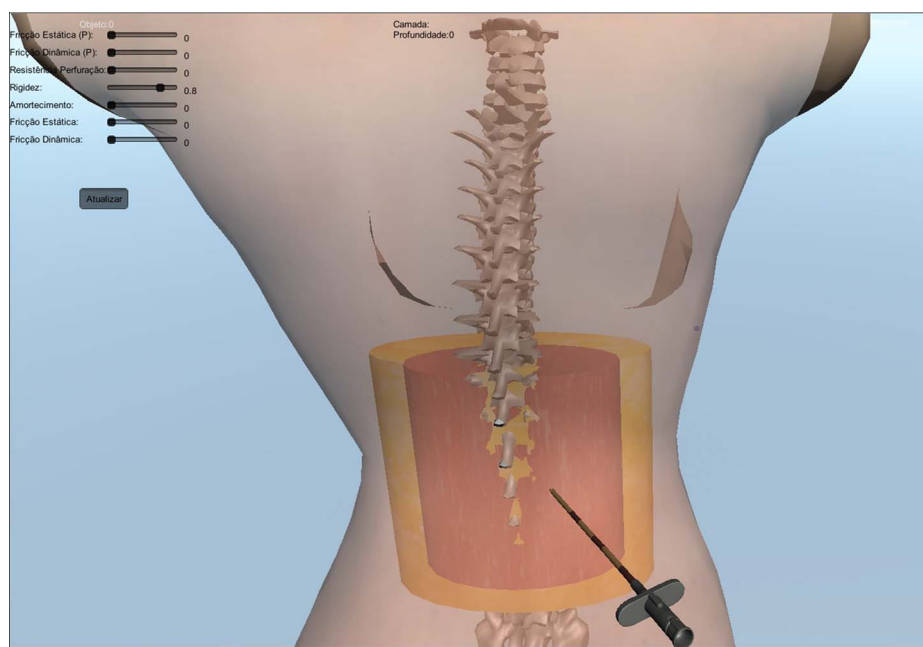


Fig. 19. Editor mode of the epidural simulator, with adjustment sliders for tissues properties.

and useful for medical skill gain on epidural practices, and pointed the need for a further implementation concerning the details of the loss of resistance (LOR) techniques on the epidural anesthesia simulator.

## 5. Conclusions

This work presented a virtual simulator supported by force models integrated to haptic feedback and gamification features. The force models consider the patient body tissues until epidural space and bone, which provides representation for answers from needle displacement in terms of axial forces for real-time feedback [16].

The current implementation includes the response of resistance forces integrated to a haptic device manipulation, by use of engine Unity3D and the Phantom Omni haptic device. The force curves achieved by use of the developed force models show that the calculated and exerted forces are similar to real experiment data [12]. Needle movement restrictions implemented inside the virtual patient body, after tissue perforation, enhance the correspondence to reality.

The needle deflection model developed considers the influence of both the needle tip shape and the needle diameter, where they significantly affect the average slope. This model was incorporated into the simulation mode, as an addition to the developed force models.

The implementation of a gamification strategy using points and achievements can be an interesting resource to keep the users practicing for a longer time, once many attempts for epidural anesthesia normally are required by trainees, to gain the skill and proficiency necessary before interaction with real patients. The gamification elements have shown a glimpse of what can be done in terms of motivation for the trainee.

The possibility of tissue properties adjustments for each tissue on

the editor mode interface facilitates medical staff experimentation, immediate adjustment and further refinement by anesthesia experts.

Future works include a plan to validate both the gamification use and the haptic feedback influence on the training of the epidural procedure, to be realized with medical community, to be able to track and compare the outcomes, the differences and possible improvements achieved in details, as well as the further adjustments needed. The planned test environments could include the following conditions: (a) only a visual feedback, (b) only a haptic device feedback, (c) both visual and haptic feedbacks, and (d) only an audio feedback. A gamification evaluation could be conducted by splitting the test users into two main groups: a group with access to the gamified environment and a second one, without this feature, to enable the mapping of the gamification effectiveness by comparison. The previous professional competence on the epidural procedure should also be considered before the tests. An accuracy and calibration of the force feedbacks based on the biomechanical properties of each epidural tissue by expert physicians, using the editor mode of the simulator is also considered. A online satisfaction survey could be filled by the simulator testers for feedback and improvement afterwards.

## Acknowledgements

A. Conci wants to thank the Conselho Nacional de Desenvolvimento Científico e Tecnológico (CNPq – <http://www.cnpq.br/>) Brazil project 303240/2015-6 and 402988/2016-7. This work is partially supported by Fundação de Amparo à Pesquisa do Estado do Rio de Janeiro (FAPERJ – [www.faperj.br](http://www.faperj.br)) Brazil project CNE 26/202.959/2016. Some implementations of this work were developed with resources of project MACC in the LNCC (Petropolis-RJ).

## References

- [1] D. Tran, K.W. Hor, A.A. Kamani, V.A. Lessoway, R.N. Rohling, Instrumentation of the loss-of-resistance technique for epidural needle insertion, *IEEE Trans. Biomed. Eng.* 56 (2009) 820–827.
- [2] M.W. Lim, G. Burt, S.V. Rutter, Use of three-dimensional animation for regional anaesthesia teaching: application to interscalene brachial plexus blockade, *Br. J. Anaesth.* 94 (2005) 372–377.
- [3] B. Maurin, L. Barbe, B. Bayle, P. Zanne, J. Gangloff, M. De Mathelin, A. Forgiione, In vivo study of forces during needle insertions, in: *Proceedings of the Medical Robotics, Navigation and Visualisation Scientific Workshop, 2004*, pp. 1–8.
- [4] N. Vaughan, V.N. Dubey, M.Y. Wee, R. Isaacs, A review of epidural simulators: where are we today? *Med. Eng. Phys.* 35 (2013) 1235–1250.
- [5] C. Crawford, *The Art of Computer Game Design*, Washington State University, Vancouver, 1984.
- [6] T. Grau, R.W. Leipold, R. Conradi, E. Martin, Ultrasound control for presumed difficult epidural puncture, *Acta Anaesthesiologica Scandinavica* 45 (2001) 766–771.
- [7] C. MacArthur, M. Lewis, E.G. Knox, Accidental dural puncture in obstetric patients and long term symptoms, *BMJ* 6882 v.306 (1993) 883–885.
- [8] L.M. Watterson, S. Hyde, S. Bajenov, S.E. Kenedy, The training environment of junior anaesthetic registrars learning epidural labour analgesia in Australian teaching hospitals, *Anaesth. Intensive Care* 1 v.35 (2007) 38.
- [9] T.P. Grantcharov, R.K. Reznik, Teaching rounds: teaching procedural skills, *BMJ* 7653 v.336 (2008) 1129–1131.
- [10] B.P. Kerfoot, N. Kissane, The use of gamification to boost residents engagement in simulation training, *JAMA Surgery* 149 (11) (2014) 1208–1209.
- [11] Sensable Technologies Inc., *OpenHaptics Toolkit Programmer's Guide - version 3.0*, Geomagic, Woburn, MA, 2009. Accessed on 14/05/2015 from link: < [http://www.geomagic.com/files/4013/4851/4367/OpenHaptics\\_ProgGuide.pdf](http://www.geomagic.com/files/4013/4851/4367/OpenHaptics_ProgGuide.pdf) > .
- [12] L. Holton, L. Hiemenz, Force models for needle insertion created from measured needle puncture data, *Stud. Health Technol. Inform.* (2001) 180–186.
- [13] A.M. Okamura, M.C. Simone, M. Leary, Force modeling for needle insertion into soft tissue, *IEEE Trans. Biomed. Eng.* 51 (2004) 1707–1716.
- [14] P.N. Brett, A.J. Harrison, T. Thomas, Schemes for the identification of tissue types and boundaries at the tool point for surgical needles, *IEEE Trans. Inf Technol. Biomed.* 4 (2000) 30–36.
- [15] N. Abolhassani, R. Patel, M. Moallem, Needle insertion into soft tissue: a survey, *Med. Eng. Phys.* 29 (2007) 413–431.
- [16] O. Gerovich, P. Marayong, A.M. Okamura, The effect of visual and haptic feedback on computer-assisted needle insertion, *Comput. Aided Surg.* 9 (2004) 243–249.
- [17] D.S. Kwon, K.U. Kyung, S.M. Kwon, J.B. Ra, H.W. Park, H.S. Kang, K.R. Cleary, Realistic force reflection in a spine biopsy simulator, *IEEE Int. Conf. Robot. Automat.* (2001) 1358–1363.
- [18] R.A. Lee, *Technical development of common anesthesiology techniques; Neuraxial anesthesia and laryngoscopy for endotracheal intubation*, TU Delft, Delft University of Technology, New Zealand, 2013.
- [19] N. Vaughan, V.N. Dubey, M.Y. Wee, R. Isaacs, Parametric model of human body shape and ligaments for patient-specific epidural simulation, *Artif. Intell. Med.* 62 (2014) 129–140.
- [20] M. Rostami, A.H.A. Yekta, P. Noormohammadpour, F. Farahbaksh, M. Kordi, R. Kordi, Relations between lateral abdominal muscles thickness, body mass index, waist circumference and skin fold thickness, *Acta Medica Iranica* 51 (2013) 101.
- [21] S.H. Smith, *An Introduction to Gamification*, HubPages: Business & Society, 2011. Accessed in 30/05/2016 from link: < <http://awesome.hubpages.com/hub/Intro-to-Gamification> > .
- [22] S. McCallum, Gamification and serious games for personalized health, *Stud. Health Technol. Inform.* 177 (2012) 85–96.
- [23] K. Huotari, J. Hamari, Defining gamification: a service marketing perspective, *Proceeding of the 16th International Academic MindTrek Conference, ACM, 2012*, pp. 17–22.
- [24] S. Deterding, Gamification: designing for motivation, *Interactions* 19 (2012) 14–17.
- [25] K. Werbach, D. Hunter, *For the Win: How Game Thinking Can Revolutionize Your Business*, Wharton Digital Press, 2012.
- [26] Z. Fitz-Walter, D. Tjondronegoro, P. Wyeth, Orientation passport: using gamification to engage university students, *Proceedings of the 23rd Australian Computer-Human Interaction Conference, ACM, 2011*, pp. 122–125.
- [27] R.L. Peiris, N. Janaka, D. De Silva, S. Nanayakkara, SHRUG: stroke haptic rehabilitation using gaming, *Proceedings of the 26th Australian Computer-Human Interaction Conference on Designing Futures: the Future of Design, ACM, 2014*, pp. 380–383.
- [28] R. Farzan, J.M. DiMicco, D.R. Millen, B. Brownholtz, W. Geyer, C. Dugan, When the experiment is over: Deploying an incentive system to all the users, in: *Symposium on Persuasive Technology, 2008*.
- [29] M. Poyade, M. Kargas, V. Portela, *Haptic Plugin for Unity 5.x.*, Digital Design Studio, Glasgow School of Art, 2015.